

Synthesis and optical properties of ZnO and carbon nanotube based coaxial heterostructures

D. S. Kim,^{1,a)} S.-M. Lee,¹ R. Scholz,¹ M. Knez,¹ U. Gösele,¹ J. Fallert,² H. Kalt,² and M. Zacharias³

¹Max Planck Institute of Microstructure Physics, Weinberg 2, 06120 Halle, Germany

²Institut für Angewandte Physik, Universität Karlsruhe, Wolfgang-Gaede-Straße 1, 76131 Karlsruhe, Germany

³IMTEK, Faculty of Applied Science, Albert-Ludwigs-University Freiburg, Georges-Köhler-Allee 103, 79110 Freiburg, Germany

(Received 22 January 2008; accepted 9 June 2008; published online 10 September 2008)

Carbon nanotubes and ZnO based functional coaxial heterostructured nanotubes have been fabricated by using atomic layer deposition. An irregular structured shell composed of ZnO nanocrystals was deposited on pristine nanotubes, while a highly defined ZnO shell was deposited on the tubes after its functionalization with Al₂O₃. Photoluminescence measurements of the ZnO shell on Al₂O₃/nanotube show a broad green band emission, whereas the shell grown on the bare nanotube shows a band shifted to the orange spectral range. © 2008 American Institute of Physics. [DOI: 10.1063/1.2952487]

Carbon nanotube (CNT) based composite materials are of particular interest because of their potential application in advanced electronics and optoelectronics. Modifications of CNTs with metal^{1,2} and semiconductor nanocrystals^{3,4} for the enhancement of optical and electrical properties of the composites have already been demonstrated. For instance, superconducting tin nanowires filled in CNTs showed a critical magnetic field more than 30 times higher than that of bulk metallic tin.⁵ CNT films when employed as conducting scaffolds in a TiO₂ based photoelectrochemical cell showed an enhancement of the photoconversion efficiency by a factor of 2.⁶

Due to the fact that ZnO is a *n*-type semiconductor with a direct wide band gap and a large exciton binding energy of 60 meV, CNTs coupled with ZnO are promising composite materials for applications in optoelectronic devices. For example, coaxial heterostructured nanotubes with a *p*-channel CNT (Ref. 7.) combined with a *n*-channel ZnO shell may be able to be integrated into logical inverters.

Various synthetic strategies based on physical and chemical processes for getting composites have been established so far.⁸ The approaches of such modifications have been reviewed in a recent review article.⁹

With the recent advance in the design of CNT composites, it is possible to coat CNTs with oxide materials by atomic layer deposition (ALD). ALD is a chemical thin film deposition method that can be used to deposit a variety of materials including oxides and metals at rather low temperatures.¹⁰ Nanotubes were coated coaxially with continuous and radially isotropic amorphous Al₂O₃ layers.¹¹ However, ZnO nanoparticles or morphologically not well-defined ZnO layers were grown on nanotubes for field-emission applications.^{12,13} For the development of promising nanoscale composite materials based on ZnO and CNTs a better understanding of the growth behavior involved in their formation is required. In this work, we fabricate coaxial nanotubes with highly defined morphologies of ZnO by em-

ploying an intermediate Al₂O₃ coating on the nanotubes using ALD. Detailed structure characterizations of the ZnO shells, which were determined by the surface properties of the templates, are presented and optical properties of the ZnO shells will be discussed as well.

CNTs [purity >60%] were obtained from Nanothinx. Al₂O₃ and ZnO shells were deposited on the nanotubes by ALD (Savannah 100, Cambridge Nanotechnology Inc.). For the synthesis of coaxially heterostructured nanotubes, a powder of CNTs was fixed by an adhesive tape on a glass substrate. Trimethylaluminum [Al(CH₃)₃], diethylzinc [Zn(C₂H₅)₂, DEZ], and H₂O were selected as the aluminum precursor, zinc precursor, and oxygen reactant sources, respectively. To optimize the growth conditions, the deposition temperature was varied from 40 to 120 °C. Shorter precursor exposure and longer purging time were attempted to achieve uniform ZnO layers, composed of small and uniform nanocrystals. Here, ZnO depositions were carried out within specific deposition temperatures, precursor exposure, and purging times. The deposition was started with a substrate temperature of 70 °C and a background pressure of 0.15 Torr. For ZnO deposition, DEZ and H₂O were alternately introduced into the ALD chamber with pulses of 0.4 and 1.5 s, respectively. An exposition time of 30 s followed by a purge time of 30 s in a 10 SCCM (SCCM denotes cubic centimeter per minute at STP) Ar flow were employed for both precursors. The shell thickness was controlled by the number of precursor/purge cycles. 50 cycles were used for the deposition of 10 nm of Al₂O₃ and 70 cycles for the deposition of 25 nm of ZnO. In the following we denote the CNT/ZnO and CNT/Al₂O₃/ZnO tube samples as type A and type B tubes for simplicity. The preparation process of type B tubes is illustrated schematically in Fig. 1.

Figure 2(a) shows a transmission electron microscopy (TEM) image of the typical morphology of CNTs prior to deposition. Most of the nanotubes are multiwall tubes. Figure 2(b) shows the typical morphology of a ZnO CNT. The deposited ZnO, composed of ZnO nanocrystals, was observed to be not uniform and discontinuous along the tube.

^{a)}Electronic mail: dskim@mpi-halle.de.



FIG. 1. (Color online) Schematic view of the fabrication process of CNTs covered by a thin Al_2O_3 layer and subsequently by a layer of ZnO (type B tube). The thickness of the ZnO and the Al_2O_3 shell is controlled by the number of ALD cycles.

Due to the chemical properties of the carbon nanotubes and the unique self-assembly characteristics of ZnO, the morphology of the ZnO shell is highly irregular. A CNT is a micromolecular form of carbon, which can be regarded as graphitic layers (sp^2 -hybridized carbon atoms) rolled up into a cylindrical form. A perfect CNT is chemically inert. However, curvature-induced pyramidalization and misalignment of the π -orbitals of the carbon atoms induce a local strain, which makes the nanotube more reactive than a flat graphene sheet.¹⁴ ZnO has a tetrahedral fundamental unit cell where the Zn ions are surrounded by O ions and vice versa, caused by the sp^3 -hybridized orbit. Since the normal direction to each plane of the tetrahedron is parallel to the c -axis, ZnO nanocrystals have a preferential orientation toward the c -axis. The existence of uncompensated polarity in ultrathin ZnO films was predicted based on first principles simulations.¹⁵ We suggest that the polarity of ZnO clusters is involved in the formation of ZnO nanocrystals. In contrast to ZnO deposition, the Al_2O_3 shells formed a uniform coat on the nanotubes. Figure 2(c) shows Al_2O_3 /CNT heterotube structures with a 10 nm amorphous Al_2O_3 shell. Even though, conformal coating of either ZnO or Al_2O_3 on CNTs was not expected since precursor molecules are unlikely to interact with the chemically inert surface of the carbon nanotube. Recently, it was suggested and demonstrated that chemical functionalization is required for uniform Al_2O_3 coating on carbon nanotubes.¹⁰ It was also predicted that DEZ molecules should become physically adsorbed on the wall of nanotubes based on first principles electronic structure calculation.¹¹ Nucleation of ZnO might be initiated at defect sites or impurities along the nanotube. However, we were able to coat the nanotubes with an Al_2O_3 shell reproducibly without any intentional pretreatment of the carbon nanotube surfaces. The necessary functionalization of the carbon nanotubes may be coming from the gas phase during sample handling. For functionalization of nanotubes certain molecules

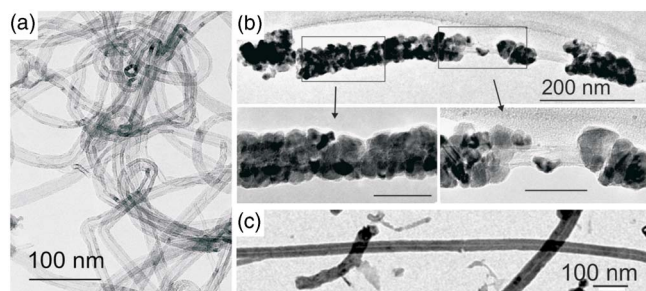


FIG. 2. (Color online) (a) TEM image of a pristine CNT. (b) TEM image of a ZnO/CNT tube. Scale bars in the enlarged images are 100 and 50 nm, respectively. (c) TEM image of a Al_2O_3 /CNT tube. Uniform coating with Al_2O_3 is visible.

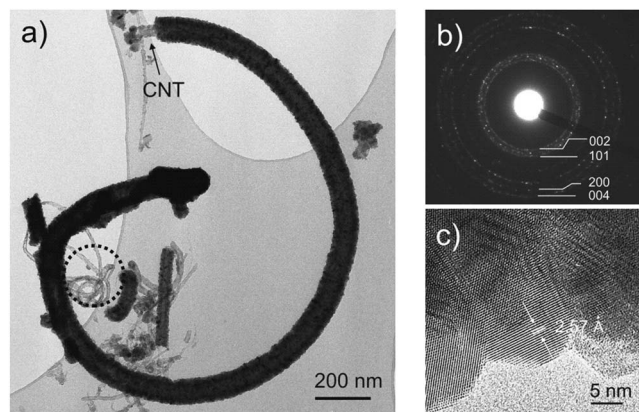


FIG. 3. (a) TEM image of a type B tube. The thin layer of Al_2O_3 is not clearly visible. Some bare CNTs, e.g., one indicated by the dotted circle, are from the core side of the powder where precursor molecules were not able to react with the CNTs. (b) SAED pattern of type B tubes. (c) HRTEM image of nanocrystalline ZnO shell of type B tube.

such as NO_2 can be used as shown by the Gordon group.¹⁰ Presumably such molecules or other chemicals which perform a similar functionalization adsorb physically from laboratory air, thus initiating an Al_2O_3 growth by ALD. However, one cannot exclude a possible chemical reaction of the precursor molecules with the nanotube wall.

Taking advantage of the homogeneous Al_2O_3 coating, we were able to deposit a well defined ZnO shell on the Al_2O_3 /CNT tubes as shown in Fig. 3(a). The thickness of the ZnO shell is ~ 25 nm. The selected area electron diffraction (SAED) pattern of the coated ZnO shell in Fig. 3(b) reveals that the structure corresponds to polycrystalline ZnO. Figure 3(c) shows a high-resolution TEM (HRTEM) image of one of these nanocrystals, in which the atomic distances confirm the hexagonal lattice.

In addition, note that the growth rates of $2 \text{ \AA}/\text{cycle}$ for Al_2O_3 and $3.5 \text{ \AA}/\text{cycle}$ for ZnO, respectively, are somewhat larger than expected for a regular ALD process. Considering the comparatively low purging time at those temperatures, it can be expected that after the water half-cycle there is still remaining water adsorbed on the CNTs, thus contributing to an additional CVD component to the ALD deposition. The water molecules, however, might contribute to the functionalization of the CNTs for the deposition process.

Figure 4 shows typical photoluminescence (PL) spectra of type A and type B tubes. The PL of the samples was measured using the 325 nm line of a HeCd laser as excitation source. Upon optical excitation above the bandgap, typically electrons and holes form quickly excitons. At room temperature the near band edge emission at ~ 3.2 eV is due to the radiative decay of free excitons and their phonon replicas. It is found in both kinds of samples that the dominant part of the emission originates from excitons which have relaxed to deeper defect states. The type A tubes showed a broad deep center luminescence peaked at ~ 2.1 eV and the type B tubes at ~ 2.5 eV. The deep level emission (DLE) may have several possible causes. Emission in the green spectral range is commonly reported in bulk ZnO and ZnO nanowires. Extrinsic impurities (Cu and Li)¹⁶ as well as intrinsic defects (oxygen vacancies)¹⁷ are discussed as responsible defects for green luminescence band. The emission in the orange spectral range is most often associated with oxygen interstitials.¹⁸

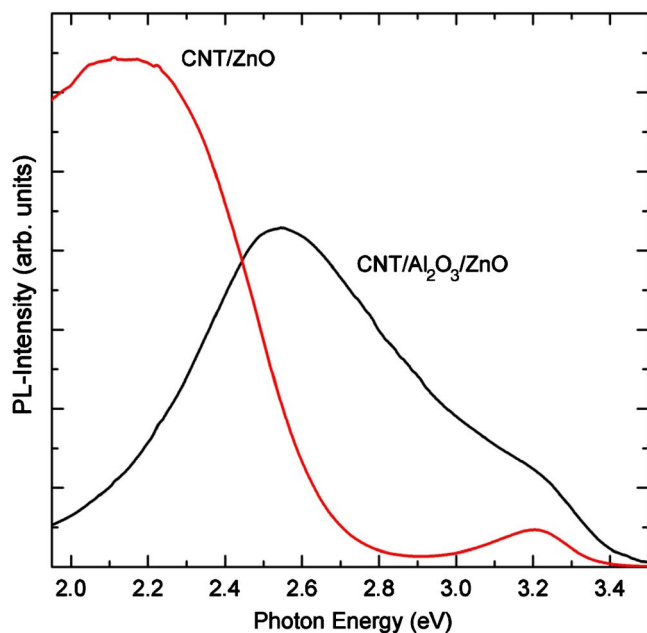


FIG. 4. (Color online) Room temperature PL spectra of CNT/ZnO (type A tubes) and CNT/Al₂O₃/ZnO tube (type B tubes).

Since the growth was performed with the identical setup without any intentional doping, the difference in the DLE between type A and B tubes is very likely caused by a different stoichiometry induced during deposition on the templates.

It is known that charge and energy transfer between a conjugated species and carbon nanotubes can occur in a photoexcited state.¹⁹ It was found that the intensity ratio of UV/visible emission of type A tubes is four times lower than that of type B tubes. This quenching could originate from a charge transfer of photoexcited electrons from ZnO to the empty electronic states of the nanotube. In type B tubes this quenching would then be suppressed by a thin layer of Al₂O₃. However, alternative reasons cannot be excluded, such as a lower quality of the ZnO shell of type A tubes.

In summary, CNTs functionalized by ZnO or Al₂O₃ shells realizing coaxial nanotubes were prepared by ALD. It was found that the morphology of the ZnO shell on nanotubes was not well defined due to the inert surface properties of the CNT template and to the unique self-assembly characteristics of ZnO. However, if an amorphous Al₂O₃ shell

was used as intermediate layer covering the nanotube, the final morphology of the ZnO shell became smooth and controllable. The comparison of the PL properties showed that the position of the DLE band of ZnO shells depends on the absence or presence of the intermediated Al₂O₃ shell.

This work was supported by the International Max Planck Research School for Science and Technology of Nanostructures (Nano-IMPRS) at Halle. S.-M.L. and M.K. greatly acknowledge the financial support by the German Federal Ministry for Education and Research (BMBF) under Contract No. 03X5507. M. Z. acknowledges the financial support by the German Research Foundation /DFG) under Contract No. Za 191/18-2.

¹B. R. Azamian, K. S. Coleman, J. J. Davis, N. Hanson, and M. L. H. Green, *Chem. Commun. (Cambridge)* **2002**, 366.

²D. S. Kim, T. Lee, and K. E. Geckeler, *Angew. Chem., Int. Ed.* **45**, 104 (2006).

³J. M. Haremza, M. A. Hahn, and T. D. Krauss, *Nano Lett.* **2**, 1253 (2002).

⁴V. Švrček, C. Pham-Huu, M.-J. Ledoux, F. Le Normand, O. Ersen, and S. Joulie, *Appl. Phys. Lett.* **88**, 033112 (2006).

⁵L. Jankovic, D. Gournis, P. N. Trikalitis, I. Arfaoui, T. Cren, P. Rudolf, M.-H. Sage, T. T. M. Palstra, B. Kooi, J. De Hosson, M. A. Karakassides, K. Dimos, A. Moukarika, and T. Bakas, *Nano Lett.* **6**, 1131 (2006).

⁶A. Kongkanand, R. Martínez Domínguez, and P. V. Kamat, *Nano Lett.* **7**, 676 (2007).

⁷R. Martel, T. Schmidt, H. R. Shea, T. Hertel, and Ph. Avouris, *Appl. Phys. Lett.* **73**, 2447 (1998).

⁸M. A. Correa-Duarte, N. Sobal, L. M. Liz-Marzan, and M. Giersig, *Adv. Mater. (Weinheim, Ger.)* **16**, 2179 (2004).

⁹D. Tasis, N. Tagmatarchis, A. Bianco, and M. Prato, *Chem. Rev. (Washington, D.C.)* **106**, 1105 (2006).

¹⁰M. Knez, K. Nielsch, and L. Niinistö, *Adv. Mater. (Weinheim, Ger.)* **19**, 3425 (2007).

¹¹D. B. Farmer and R. G. Gordon, *Nano Lett.* **6**, 699 (2006).

¹²Y.-S. Min, E. J. Bae, J. B. Park, U. J. Kim, W. Park, J. Song, C. S. Hwang, and N. Park, *Appl. Phys. Lett.* **90**, 263104 (2007).

¹³J. M. Green, L. Dong, T. Gutu, J. Jiao, J. F. Conley, Jr., and Y. Ono, *J. Appl. Phys.* **99**, 094308 (2006).

¹⁴S. Niyogi, M. A. Hamon, J. Hu, B. Zhao, P. Bhowmik, R. Sen, M. E. Itkis, and R. C. Haddon, *Acc. Chem. Res.* **35**, 1105 (2002).

¹⁵J. Goniakowski, C. Noguera, and L. Giordano, *Phys. Rev. Lett.* **98**, 205701 (2007).

¹⁶R. Dingle, *Phys. Rev. Lett.* **23**, 579 (1969).

¹⁷F. H. Leiter, H. R. Alves, A. Hofstaetter, D. M. Hofmann, and B. K. Meyer, *Phys. Status Solidi B* **226**, R4 (2001).

¹⁸S. A. Studenikin, N. Golego, and M. Cocivera, *J. Appl. Phys.* **84**, 2287 (1998).

¹⁹H. Ago, M. S. P. Shaffer, D. S. Ginger, A. H. Windle, and R. H. Friend, *Phys. Rev. B* **61**, 2286 (2000).